High-resolution photoelectron spectrum of the origin band of the X̃+2E ← X̃1A1 ionising transition of propyne

Author(s):
Jacovella, Ugo; Merkt, Frédéric

Publication date:
2018

Permanent link:
https://doi.org/10.3929/ethz-b-000314261

Originally published in:
Molecular Physics 116(23-24), https://doi.org/10.1080/00268976.2018.1451002

Funding acknowledgement:
172620 - Precision measurements with cold molecules: Rydberg states, ions and photoionization (SNF)

High-resolution photoelectron spectrum of the origin band of the $\tilde{X}^+\ ^2E \leftarrow \tilde{X}\ ^1A_1$ ionizing transition of propyne

U. Jacovella[a] and F. Merkt[a]

[a]Laboratory of Physical Chemistry, ETH Zurich, CH-8093 Zurich, Switzerland

ARTICLE HISTORY
Compiled November 19, 2019

ABSTRACT
The PFI-ZEKE photoelectron spectrum of the origin band of the $\tilde{X}^+\ ^2E \leftarrow \tilde{X}\ ^1A_1$ ionizing transition of propyne has been recorded at a resolution sufficient to partially resolve the rotational structure. The rovibronic photoionization selection rules are derived in the spin double group $C_{3v}(MS)^2$ and are used to model the experimental spectrum and determine the adiabatic ionization energy of propyne and the spin-orbit coupling constant of the radical cation of propyne. The Jahn-Teller effect is found to significantly affect the spin-orbit splitting of the cationic ground state.

KEYWORDS
PFI-ZEKE photoelectron spectroscopy; Propyne radical cation; Jahn-Teller effect; spin-orbit coupling;

1. Introduction

Propyne (H–CC–CH_3) and its cation play an important role as intermediates in combustion processes [1] and astrochemistry [2, 3]. The ground electronic state of H–CC–CH_3^+ is formed upon removal of an electron out of the doubly degenerate outer-valence-shell molecular orbital (e symmetry, C≡C-triple-bond π character) of propyne. Therefore, the propyne radical cation has a doubly degenerate ground electronic state ($\tilde{X}^+\ ^2E$ in the $C_{3v}(MS)$ group), which implies the simultaneous occurence of the Jahn-Teller (JT) effect and spin-orbit coupling, as in the case of the radical cation of 2-butyne [4]. The highest occupied molecular orbital (HOMO) of propyne resembles that of acetylene and 2-butyne, and the electron-hole probability density is mainly located on the CC triple bond. In the case of acetylene, the molecular cation is linear, and the Renner-Teller effect does not significantly affect the ground vibronic state, which is split into two spin-orbit components separated by $A_{so}^+ = -30.86(44)$ cm^{-1} [5], where the negative sign indicates an inverted order with the $^2\Pi_{3/2}$ component lying below the $^2\Pi_{1/2}$ component. In the case of 2-butyne, the equilibrium structure of the cation is slightly distorted by the JT effect, which reduces the spin-orbit splitting to a value of $A_{so}^+ = -10.5(10)$ cm^{-1} [4]. A similar reduction of the spin-orbit splitting is also expected in the ground-state of the radical cation of propyne [6] and was indeed observed [7, 8], as discussed below.

The information on the propyne radical cation in the gas phase available in the

CONTACT F. Merkt. Email: frederic.merkt@phys.chem.ethz.ch

literature comes almost exclusively from studies by photoionization and photoelectron spectroscopy [7–13]. The He I and threshold photoelectron spectra [9–12] contain information on the vibrational structure of the $\tilde{X}^+$ state, and consist of a strong origin band and of short and weak vibrational progressions in the C≡C and C–C stretching modes. This observation indicates that the equilibrium structure of the cationic ground state is similar to that of the neutral ground state and that the JT effect is weak. No information on the spin-orbit coupling constant, nor on the rotational structure could be derived from these spectra.

Matsui *et al.* [13] recorded the photoelectron spectrum of propyne at higher resolution by nonresonant two-photon pulsed-field-ionization zero-kinetic-energy (PFI-ZEKE) photoelectron spectroscopy and could observe the rotational envelope of the origin band, from which they concluded that the spin-orbit coupling constant of the cationic ground state is comparable to that of HC_2H^+, which in turn implies a very weak JT effect. Shieh *et al.* [7] have recorded the 2+1 resonance-enhanced multiphoton ionization (REMPI) spectrum of propyne and obtained information on several Rydberg series of propyne. By extrapolating these series, they concluded that the spin-orbit splitting of the ground vibronic state of H–CC–CH_3^+ is reduced compared to HC_2H^+ and that the energetical order of the spin-orbit components is regular, i.e., with the $E_{1/2}$ component lying below the $E_{3/2}$ component. The reduction of the strength of the spin-orbit interaction compared to HC_2H^+ suggests that the JT effect may play a more significant role in the ground state of H–CC–CH_3^+ than estimated by Matsui *et al.* [13].

More recently, Xing *et al.* [8] have measured the resonant two-photon $(1+1')$ PFI-ZEKE photoelectron spectrum of the $\tilde{X}^+\ ^2E, \nu_1^+ = 1$ cationic state via the $\tilde{X}\ ^1A_1, \nu_1 = 1$ intermediate level of propyne (ν_1 and ν_1^+ are the C–H symmetric-stretching modes of the neutral and ionized species, respectively). They also recorded the single-photon PFI-ZEKE photoelectron spectrum of the $\tilde{X}^+ \leftarrow \tilde{X}$ band of propyne at a resolution of 1.5 cm^{-1}. From the analysis of the rotational envelope of this band (see their Fig. 1), they determined the spin-orbit coupling splitting to be $A_{so}^+ = -13.0(2)$ cm^{-1} [8], which has the same absolute value as the value determined by Shieh *et al.* [7], but the opposite sign. However, they reported that the $E_{1/2}$ component lies below the $E_{3/2}$ component, which is characteristic of a normal order and a positive value of A_{so}^+. Their analysis of the intensity distributions of the photoelectron spectrum was based on rovibrational photoionization selection rules in the C_{3v}(MS) group and not the spin double group, as would be appropriate for a molecule exhibiting a measurable spin-orbit splitting. The 60 % reduction of the spin-orbit splitting observed by Xing *et al.* compared to HC_2H^+ indicates that the JT effect is strong enough to significantly quench the spin-orbit coupling and contradicts the observation made by Matsui *et al.* [13].

The conclusions drawn on the relative strength of the JT and spin-orbit coupling and on the sign of the spin-orbit coupling in Refs. [7, 8, 13] are incompatible. To clarify the situation, Marquez *et al.* [6] performed high-level *ab initio* calculations including vibronic and spin-orbit interactions. They calculated the pure electronic spin-orbit coupling interaction of the propyne radical cation to be $a\zeta_e = -28$ cm^{-1}, a value that does not take into account the JT interaction but only the reduction of the electronic-spin density on the C atoms in the propyne cation. After inclusion of the JT interaction, the spin-orbit splitting was found to be reduced to $A_{so}^+ = a\zeta_e d = -18$ cm^{-1} [6], a result that is in qualitative agreement with the results of Xing *et al.* [8] and Shieh *et al.* [7] if the sign is ignored.

Here, we present the single-photon PFI-ZEKE photoelectron spectrum of the

$\tilde{X}^+ \leftarrow \tilde{X}$ photoionizing transition of propyne recorded at a resolution of ~ 0.8 cm^{-1}. This resolution enabled us to partially resolve the rotational structure of the origin band of the photoelectron spectrum. Its analysis was carried out in the $C_{3v}(MS)^2$ spin double group corresponding to a Hund's case (a)-type description of the cationic state.

2. Experimental procedure

The PFI-ZEKE photoelectron spectrum of propyne was recorded using the broadly tunable vacuum-ultraviolet (VUV) laser system and PFI-ZEKE photoelectron spectrometer described in Ref. [5].

A pulsed valve was used to introduce the gas mixture, consisting of 10 % C_3H_4 in Ar, into the vacuum chamber. The nozzle stagnation pressure was set at 2 bar to ensure the production of a supersonic beam. The coldest part of the supersonic beam, corresponding to a rotational temperature of about 8 K, was selected by a skimmer before entering the photoexcitation region, where it crossed the VUV laser beam at right angles.

The VUV laser radiation ($\tilde{\nu}_{\mathrm{VUV}} = 2\tilde{\nu}_1 - \tilde{\nu}_2$) in the region of the adiabatic ionization threshold of propyne ($\approx 83\,650$ cm^{-1}) was generated by resonance-enhanced difference-frequency mixing in a gas jet of Kr using the $4p^5 5p'[1/2]_0 \leftarrow 4p^6\ {}^1S_0$ two-photon resonance at $2\tilde{\nu}_1 = 98\,855.071$ cm^{-1}. The VUV wavenumber was scanned by changing $\tilde{\nu}_2$. The wavenumber calibration was carried out at an absolute accuracy of 0.2 cm^{-1} using a wavelength meter to determine $\tilde{\nu}_1$ and $\tilde{\nu}_2$.

The PFI-ZEKE photoelectron spectra were recorded by monitoring the electron signal produced by the pulsed field ionization of high Rydberg states located below the rovibronic ionization thresholds [14]. To this end, an electric-field pulse sequence consisting of a discrimination pulse of 167 mV/cm followed by a field-ionization pulse of -333 mV/cm was used, resulting in a spectral resolution of 0.8 cm^{-1}. The positions of the field-free ionization thresholds were obtained by correcting for the shifts induced by the field ionization, as explained in Ref. [15].

3. Experimental results

The PFI-ZEKE photoelectron spectrum of the origin band of the $\tilde{X}^+ \leftarrow \tilde{X}$ photoionizing transition of propyne is depicted in panel a of Fig. 1, where it is compared to a spectrum calculated on the basis of a model of the rotational structure described below (panel d). Panels b and c of Fig. 1 depict the contributions to the spectrum calculated for the lower ($\Omega = 3/2$) and the upper ($\Omega = 1/2$) spin-orbit components of the propyne radical cation, respectively. The spectrum consists of a strong, broad, and only partially resolved feature on its low-wavenumber side and of three much weaker bands on its high-wavenumber side.

To analyze the rotational structure, the rotational level energies of neutral propyne were calculated using the standard expression for a prolate symmetric top ($A > B \simeq C$)

$$\frac{E_{N''K''}}{hc} = BN''(N''+1) + (A-B)K'', \tag{1}$$

where N'' is the rotational quantum number and K'' is the quantum number associated

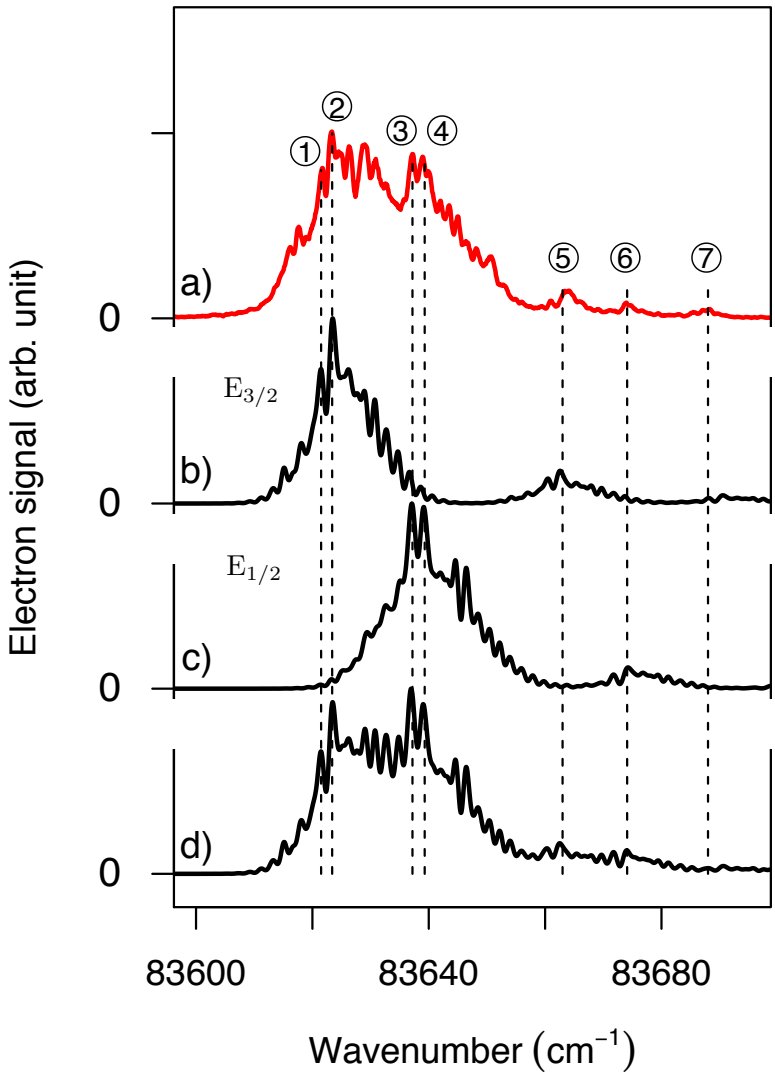

Figure 1. a) Rotational structure of the origin band of the PFI-ZEKE photoelectron spectrum of the $\tilde{X}^+\ ^2E \leftarrow \tilde{X}\ ^1A_1$ photoionizing transition of propyne and model calculations of the contributions expected for the transition to the lower spin-orbit component ($E_{3/2}$, trace b) and the transition to the upper spin-orbit component ($E_{1/2}$, trace c). Trace d is a weighted sum of these contributions (see text).

with the projection of $\vec{N}''$ onto the top axis (a axis). At the low rotational temperature of the sample in the supersonic beam centrifugal-distortion effects are negligible. The rotational level energies of the cation were calculated using the effective Hamiltonian derived by Brown for symmetric-top molecules in ^2E states with spin-orbit and JT interactions [16]

$$\begin{aligned}\frac{E_{J^+p^+}}{hc} =& B^+J^+(J^+ + 1) + (A^+ - B^+)p^{+2} \\ & - 2A^+p^+\zeta_{ev} + A^+\zeta_{ev}^2 \\ & - 2A^+p^+\sigma^+ + 2A^+\sigma^+\zeta_{ev} + \frac{B^+}{2} + \frac{A^+}{4} + a\zeta_e d\sigma^+.\end{aligned} \tag{2}$$

In Eq. (2), J^+ is the total angular-momentum quantum number excluding nuclear spins, $p^+ = k^+ + \sigma^+$ is the quantum number associated with the projection of $\vec{J^+}$ on the top axis, and k^+ and σ^+ are the quantum numbers for the projection of the rotational angular momentum and the electronic spin, respectively. p^+, k^+ and σ^+ are signed quantities. $a\zeta_e d$ is an effective spin-orbit coupling constant which includes a pure electronic factor, $a\zeta_e$, and a reduction factor d from the JT effect, and ζ_{ev} is an effective vibronic Coriolis coupling term (see Refs. [16–19]). In the ground vibronic state of H–CC–CH_3^+, and assuming a single dominant JT-active mode, ζ_{ev} can be approximated by [16, 17]

$$\zeta_{ev} = \zeta_e d + \frac{1}{2}\zeta_{i_1,i_2}(1-d), \tag{3}$$

where ζ_{i_1,i_2} describes the Coriolis coupling of the two components (i_1 and i_2) of the JT-active mode.

The general rovibronic photoionization selection rules [20]

$$\Gamma''_{rve} \otimes \Gamma^+_{rves} \supset \Gamma^* \qquad \text{for } \ell \text{ even}, \tag{4}$$

$$\Gamma''_{rve} \otimes \Gamma^+_{rves} \supset \Gamma^{(s)} \qquad \text{for } \ell \text{ odd}, \tag{5}$$

are used to determine the allowed photoionization transitions. In Eqs. (4) and (5), Γ''_{rve} and Γ^+_{rves} are the symmetry of the rovibronic levels of neutral propyne and of the spin-rovibronic levels of the cation of propyne, respectively, and ℓ is the orbital-angular momentum quantum number of the photoelectron partial wave. To classify the energy levels, we use the $C_{3v}(MS)^2$ spin double group, the character table of which is given in Table 1. $\Gamma^* = A_2$ and $\Gamma^{(s)} = A_1$ are the representations of the dipole-moment and identity operation, respectively (see Table 1).

Table 1. Character table of the $C_{3v}(MS)^2$ group, taken from Ref. [21].

$C_{3v}(MS)^2$	E	(123)	$(23)^*$	R	R(123)	
	1	2	6	1	2	
Equiv. rot.	R^0	$R_z^{\pi/2}$	$R_{\pi/2}^{\pi}$	$R^{2\pi}$	$R_z^{8\pi/2}$	
A_1	1	1	1	1	1	$\Gamma^{(s)}$
A_2	1	1	−1	1	1	Γ^*
E	2	−1	0	2	−1	
$E_{1/2}$	2	1	0	−2	−1	
$E_{3/2}$	2	−2	0	−2	2	

The selection rules (4) and (5) applied in the $C_{3v}(MS)^2$ group lead to the transitions summarized in Table 2. The transitions predicted for even and odd ℓ values are the same because $A_1 \otimes E = A_2 \otimes E = E$ and $E \otimes E = A_1 \oplus A_2 \oplus E$.

The rovibronic symmetries of the rotational levels of neutral propyne are A_1 for $K'' = 0$, J'' = even; A_2 for $K'' = 0$, J'' = odd; E for $K'' = |3n \pm 1|$ with $n = 0, 1, 2, ...$ and $A_1 \oplus A_2$ for $K'' = 3n$ with $n = 1, 2, ...$. For the cation, they are $E_{1/2}$ for $P^+ = |p^+| = |3n \pm 1/2|$ with $n = 0, 1, 2, ...$, and $E_{3/2}$ for $P^+ = |3n \pm 3/2|$ with $n = 0, 1, 2, ...$. At the rotational temperature of 8 K, only levels with $K'' = 0$ and 1 are significantly populated in the ground neutral state.

A single-center expansion of the HOMO of propyne is dominated by p_π and d_π contributions, where the index π indicates a projection of $\pm\hbar$ of the orbital angular mo-

Table 2. Allowed rovibronic transitions in the origin band of the $\tilde{X}^+\ ^2E \leftarrow \tilde{X}\ ^1A_1$ photoionizing transition of propyne (Γ^+_{ve}= E $\leftarrow \Gamma''_{ve} = A_1$).

Γ''_{rve}		Γ^+_{ves}	Γ^+_r	Γ^+_{rves}
A_1/A_2	$\rightarrow$	$E_{3/2} \otimes$	$E_{3/2}$	$A_1 \oplus A_2$
	$\rightarrow$	$E_{1/2} \otimes$	$E_{1/2}$	$A_1 \oplus A_2 \oplus E$
E	$\rightarrow$	$E_{3/2} \otimes$	$E_{1/2}$	E
	$\rightarrow$	$E_{1/2} \otimes$	$E_{3/2}$	E
		$\otimes$	$E_{1/2}$	$A_1 \oplus A_2 \oplus E$

mentum along the top axis (a axis). Consequently, both even- and odd-ℓ photoelectron partial waves with $\ell \leq 3$ must be considered when deriving the allowed photoionizing transitions. Angular-momentum conservation implies that photoionization out of the HOMO leads to the selection rules $\Delta J = J^+ - J'' = \pm 1/2, \pm 3/2, \pm 5/2, \pm 7/2$, and $\pm 9/2$, and $K^+ - K'' = \pm 1$. Applying a simple orbital ionization model following Hund's angular-momentum coupling case (a), one obtains additional selection rules on Δp ($\Delta p = p^+ - k''$): $\Delta p = +3/2$ for the $E_{3/2}$ spin-orbit component and $\Delta p = -1/2$ for the $E_{1/2}$ spin-orbit component. Additionally, two weaker contributions are expected to be observable and responsible for satellite bands with $\Delta p = -3/2$ for the $E_{3/2}$ spin-orbit component and $\Delta p = -5/2$ for the $E_{1/2}$ spin-orbit component (See Ref. [22] for a detailed discussion of this selection rule).

The main features in the calculated spectrum of the lower spin-orbit component ($E_{3/2}$) presented in Fig. 1b arise from three strong and overlapping $\Delta p = +3/2$ subbands ($k'' = 0 \rightarrow p^+ = 3/2$, $k'' = 1 \rightarrow p^+ = 5/2$, and $k'' = -1 \rightarrow p^+ = 1/2$). The main feature of the calculated spectrum of the upper spin-orbit component (Fig. 1c) originate from three overlapping $\Delta p = -1/2$ subbands ($k'' = 0 \rightarrow p^+ = -1/2$, $k'' = 1 \rightarrow p^+ = 1/2$, $k'' = -1 \rightarrow p^+ = -3/2$). For both spin-orbit components, rotational branches with $|\Delta J| = 1/2$, 3/2, 5/2, and 7/2 were weighted by the empirical factors of 1, 1, 0.8, and 0.6, respectively. Moreover, the relative overall intensity of the transitions to the $\Omega = 1/2$ component was weighted by an additional empirical factor of 0.75 to best reproduce the experimental photoelectron spectrum. This factor accounts for the fact that Rydberg series converging to the upper spin-orbit component of the cation ($E_{1/2}$) contribute to the intensity of the PFI-ZEKE photoelectron spectrum of the lower component ($E_{3/2}$) through channel interactions [23]. In the absence of such interactions, the transitions of the two spin-orbit components should have equal intensities, as explained by Marquez *et al.* [6].

The facts that the rotational structure is only partially resolved and that several molecular constants are correlated in the Hamiltonian of the cation render the analysis challenging. To reduce the ambiguities, the following procedure was followed. First, we fixed A^+ and B^+ to the values obtained from *ab initio* calculations [6], i.e., 5.24 cm^{-1} and 0.275 cm^{-1}, respectively, and adjusted ζ_{ev} to best reproduce the positions of the satellite bands labeled 5, 6 and 7 in Fig. 1a. Band 5 corresponds to transitions originating from $k'' = 0$ levels to $p^+ = -3/2$ levels of the $E_{3/2}$ spin-orbit component, Band 7 to transitions originating from $k'' = -1$ levels to $p^+ = -5/2$ levels of the $E_{3/2}$ spin-orbit component, and Band 6 transitions originating from $k'' = 0$ levels to $p^+ = -5/2$ levels of the $E_{1/2}$ spin-orbit component. From these three satellite bands, we determined ζ_{ev} to be 0.74(10).

The features labeled 1 and 2 were then assigned to transitions from the $k'' = 0$ levels to the $p^+ = 3/2$ levels of the lower spin-orbit component ($E_{3/2}$) with the selection rule $\Delta J = -1/2$ and $+1/2$, respectively. The features labeled 3 and 4 correspond to

transition from $k'' = 0$ levels to $p^+ = -1/2$ levels of the upper spin-orbit component ($E_{1/2}$) with the selection rule $\Delta J = -1/2$ and $+1/2$, respectively. From these four branches, the effective spin-orbit coupling constant $A_{so} = a\zeta_e d$ was determined to be $-12.6(20)$ cm^{-1}. Using the pure electronic spin-orbit constant $a\zeta_e$ obtained by Marquez *et al.* [6] ($a\zeta_e = -28$ cm^{-1}), a d value of 0.45 reproduces the experimental photoelectron spectrum best. The analysis also resulted in an improved value of the adiabatic ionization energy of $E_{I,ad} = 83\,623.6(20)$ cm^{-1} of propyne. Our effective spin-orbit coupling constant ($A_{so} = -12.6(20)$ cm^{-1}) is compatible with the value reported by Xing *et al.* [8] ($A_{so} = -13.0(2)$ cm^{-1}), although they appear to have treated the level structure of the cation in Hund's case (b) and to have come to the conclusion that the $E_{1/2}$ level lies below the $E_{3/2}$ level (see above), in contrast to our findings. Their value of the adiabatic ionization energy ($E_{I,ad} = 83\,619.0(10)$ cm^{-1} [8]) lies slightly below our value, which can be explained by the different treatments of the rotational structure.

4. Conclusions

The high-resolution PFI-ZEKE photoelectron spectrum of propyne has been recorded following single-photon excitation from the ground neutral state. The analysis of weak satellite bands have allowed the determination of the effective vibronic Coriolis coupling factor, $\zeta_{ev} = 0.74(10)$ for the vibronic ground state of H–CC–CH_3^+, which differs from the product $\zeta_e d$ (≈ 0.45). This observation suggests an important contribution from the second term on the right hand side of Eq. (3) to ζ_{ev} [17] and may also reflect the approximate nature of this equation. The most intense features observed in the PFI-ZEKE photoelectron spectrum have been used to extract the effective spin-orbit coupling constant of the propyne cation, $A_{so} = a\zeta_e d = -12.6(20)$ cm^{-1} and the value of the adiabatic ionization energy of propyne, $E_{I,ad} = 83\,623.6(20)$ cm^{-1}.

Acknowledgement

This work is supported financially by the Swiss National Science Foundation under project Nr. 200020-172620.

Disclosure statement

No potential conflict of interest was reported by the authors.

References

[1] N. Hansen, J.A. Miller, P.R. Westmoreland, T. Kasper, K. Kohse-Höinghaus, J. Wang and T.A. Cool, Combust. Flame **156**, 2153 – 2164 (2009).
[2] A. Coustenis, A. Salama, B. Schulz, S. Ott, E. Lellouch, T. Encrenaz, D. Gautier and H. Feuchtgruber, Icarus **161**, 383 – 403 (2003).
[3] R.I. Kaiser, D.S. Parker and A.M. Mebel, Annu. Rev. Phys. Chem. **66**, 43–67 (2015).
[4] U. Jacovella, B. Gans and F. Merkt, Mol. Phys. **113**, 2115–2124 (2015).
[5] P. Rupper and F. Merkt, Rev. Sci. Instr. **75**, 613–622 (2004).

[6] S. Marquez, J. Dillon and D.R. Yarkony, J. Phys. Chem. A **117**, 154303 (2013).
[7] J.C. Shieh, J. lin Chang, J.C. Wu, R. Li, A.M. Mebel, N.C. Handy and Y.T. Chen, J. Chem. Phys. **112**, 7384–7393 (2000).
[8] X. Xing, M.K. Bahng, B. Reed, C.S. Lam, K.C. Lau and C.Y. Ng, J. Chem. Phys. **128**, 094311 (2008).
[9] C. Baker and D.W. Turner, Proc. R. Soc. London, Ser. A **308**, 19–37 (1968).
[10] W. Ensslin, H. Bock and G. Becker, J. Am. Chem. Soc. **96**, 2757–2762 (1974).
[11] A.C. Parr, A.J. Jason, R. Stockbauer and K. McCulloh, Int. J. Mass Spectrom. **30**, 319 – 330 (1979).
[12] G.H. Ho, M.S. Lin, Y.L. Wang and T.W. Chang, J. Chem. Phys. **109**, 5868–5879 (1998).
[13] H. Matsui, Y.F. Zhu and E.R. Grant, Laser Chem. **16**, 151–156 (1996).
[14] K. Müller-Dethlefs and E.W. Schlag, Ann. Rev. Phys. Chem. **42**, 109–136 (1991).
[15] U. Hollenstein, R. Seiler, H. Schmutz, M. Andrist and F. Merkt, J. Chem. Phys. **115**, 5461–5469 (2001).
[16] J.M. Brown, Mol. Phys. **20**, 817–834 (1971).
[17] M.S. Child and H.C. Longuet-Higgins, Phil. Trans. R. Soc. London Ser. A **254**, 259–294 (1961).
[18] X. Liu, C.P. Damo, T.Y.D. Lin, S.C. Foster, P. Misra, L. Yu and T.A. Miller, J. Phys. Chem. **93**, 2266–2275 (1989).
[19] T.A. Barckholtz and T.A. Miller, Int. Rev. Phys. Chem. **17**, 435–524 (1998).
[20] R. Signorell and F. Merkt, Mol. Phys. **92**, 793–804 (1997).
[21] P.R. Bunker and P. Jensen, *Molecular Symmetry and Spectroscopy*, 2nd ed. (NRC Resaerch Press, Otawa, Ontario, Canada, 1998).
[22] M. Grütter, J.M. Michaud and F. Merkt, J. Chem. Phys. **134**, 054308 (2011).
[23] F. Merkt and T.P. Softley, Int. Rev. Phys. Chem. **12**, 205–239 (1993).